

1 Structure and reconstitution of a hydrolase complex that releases
2 peptidoglycan from the membrane after polymerization

3
4 Authors: Kaitlin Schaefer,^{1‡} Tristan W. Owens,^{2‡} Julia E. Page,¹ Marina Santiago,¹
5 Daniel Kahne,² Suzanne Walker^{1*}

6
7
8 Affiliations:

9 ¹ Department of Microbiology, Harvard Medical School, Boston, Massachusetts 02115

10 ² Department of Chemistry and Chemical Biology, Harvard University, Cambridge,
11 Massachusetts 02138

12
13 ‡ These authors contributed equally.

14 *Correspondence to: suzanne_walker@hms.harvard.edu

15

16

17 **Bacteria are surrounded by a peptidoglycan cell wall that is essential for**
18 **their survival¹. During cell wall assembly, a lipid-linked disaccharide-peptide**
19 **precursor called Lipid II is polymerized and crosslinked to produce mature**
20 **peptidoglycan. As Lipid II is polymerized, nascent polymers remain membrane-**
21 **anchored at one end and the other end becomes crosslinked to the matrix²⁻⁴. A**
22 **longstanding question is how bacteria release newly synthesized peptidoglycan**
23 **strands from the membrane to complete the synthesis of mature peptidoglycan.**
24 **Here we show that a *Staphylococcus aureus* cell wall hydrolase and a membrane**
25 **protein containing eight transmembrane helices form a complex that acts as a**
26 **peptidoglycan release factor. The complex cleaves nascent peptidoglycan**
27 **internally to produce free oligomers as well as lipid-linked oligomers that can**
28 **undergo further elongation. The polytopic membrane protein, which is similar to a**
29 **eukaryotic CAAX protease, controls the length of these products. A 2.6 Å**
30 **resolution structure of the complex shows that the membrane protein scaffolds the**
31 **hydrolase to orient its active site for cleavage of the glycan strand. We propose**
32 **that this complex serves to detach newly-synthesized peptidoglycan polymer from**
33 **the cell membrane to complete integration into the cell wall matrix.**

34

35 The biosynthesis of the bacterial cell wall has been the focus of intense study for
36 decades.¹ The peptidoglycan precursor Lipid II is synthesized inside the cell, transported
37 across the cytoplasmic membrane,^{5,6} and then assembled outside the cell into a
38 crosslinked polymer that prevents osmotic lysis (Fig. 1a, left and middle panel)². Two
39 conserved families of peptidoglycan synthases carry out Lipid II polymerization and
40 crosslinking²⁻⁴. These peptidoglycan synthases, particularly the transpeptidase (TP)
41 components, have received a great deal of attention as targets for antibiotics. Indeed,
42 transpeptidases are generically known as penicillin-binding proteins because they react
43 covalently with beta-lactam antibiotics (PBPs)⁷. A necessary step in peptidoglycan
44 biosynthesis that has received almost no attention is the release of newly synthesized
45 peptidoglycan strands from the membrane (Fig. 1a, right panel). One way in which this

46 might be achieved is with a glycosidase that cleaves within a glycan strand to separate
47 the end that has been crosslinked into the cell wall from the lipid-linked nascent oligomer
48 that is not yet crosslinked.⁸ Here, we describe a membrane protein complex comprising
49 a glycosidase and a membrane protein that regulates its cleavage activity. This complex
50 meets criteria for a peptidoglycan release factor and explains how nascent peptidoglycan
51 is freed from the membrane in *S. aureus*.

52 To find genes important in cell wall assembly, we probed a *S. aureus* transposon
53 library with sublethal concentrations of three different beta-lactams that have distinct PBP
54 inhibition profiles (Fig. 1b)⁹⁻¹¹. For *sagB*, encoding a membrane-anchored
55 glucosaminidase that affects peptidoglycan strand length¹²⁻¹⁴, we observed an unusual
56 response pattern in that transposon reads were strongly depleted in the presence of
57 oxacillin and mecillinam, but enriched in the presence of cefoxitin (Fig. 1b; Supplementary
58 Table 1). Only one other gene displayed the same pattern: *spdC*, encoding a membrane
59 protein similar to eukaryotic CAAX proteases, enzymes that cleave prenylated proteins
60 C-terminal to the site of prenylation. CAAX protease homologs are widespread in
61 bacteria, but their roles have been unclear because protein prenylation is a modification
62 not found in bacteria. Notably, *sagB* and *spdC* knockouts were reported in separate
63 studies to share several distinctive phenotypes^{12,13,15,16}. Together with the shared Tn-seq
64 profiles, these joint phenotypes led us to think SagB and SpdC may act in a complex.

65 To test whether SagB and SpdC form a complex, we expressed Myc-SpdC in *S.*
66 *aureus* $\Delta spdC$ and immunoprecipitated the tagged protein from solubilized membranes.
67 Polyacrylamide gel electrophoresis (PAGE) of the sample showed a band that contained
68 SagB as a major component (Fig. 1c; Supplementary Fig. 1, Supplementary Table 2).
69 Based on this finding, we co-expressed SagB-His₆ and FLAG-SpdC in *E. coli* and purified
70 a complex containing SpdC and SagB in a 1:1 ratio (Fig. 1c, and also see Supplementary
71 Fig. 2). *S. aureus* contains only one other glucosaminidase with a transmembrane helix,
72 SagA.^{12,13} The protein is homologous to SagB but did not have the same profile in our
73 Tn-seq experiments, and we were unable to copurify SpdC with SagA (Supplementary
74 Fig. 3). Taken together, our experiments showed that SpdC and SagB form a stable,
75 specific complex.

76 To determine whether SpdC affects SagB activity, we compared the cleavage
77 activity of the complex and SagB alone. We incubated the enzyme or enzyme complex
78 with uncrosslinked peptidoglycan prepared in vitro from synthetic [¹⁴C]-Lipid II¹⁷⁻¹⁹ and
79 analyzed the reactions via PAGE-autoradiography (Fig. 2, and see Supplementary Fig.
80 4). Consistent with previous findings, SagB lacking its TM helix has low activity (Fig. 2b,
81 lane 6; also Supplementary Fig. 5)^{13,20}. In contrast, full-length SagB fully converted the
82 peptidoglycan oligomers to diffuse bands high in the gel (Fig. 2b, lane 4). SagA produced
83 similar product bands. These were found to be short cleavage products ranging from two
84 to eight sugars in length (Supplementary Fig. 6). The SagB-SpdC complex also produced
85 short oligosaccharides, but they were longer on average than those produced by SagB
86 alone (Supplementary Fig. 6); moreover, we observed an accumulation of faster-
87 migrating cleavage products not observed for SagB alone (Fig. 2b). We observed a
88 similar accumulation of fast-migrating products when the native *S. aureus* substrate was
89 used to make peptidoglycan polymer (Supplementary Fig. 7).

90 We next sought to identify the cleavage fragments that uniquely accumulate for
91 the SagB-SpdC complex. Their migration behavior suggested these fragments may still

92 contain the diphospholipid anchor at the reducing end. Because peptidoglycan
93 glycosyltransferases (GTs) add Lipid II to the reducing end of the growing polymer²¹⁻²³,
94 one way to test if the SagB-SpdC cleavage products retain the diphospholipid is to
95 determine whether they are competent substrates for polymer extension (Fig. 2d).
96 Therefore, we prepared radiolabeled peptidoglycan oligomers, cleaved them with SagB-
97 SpdC, incubated the cleavage products with *S. aureus* PBP2 and cold Lipid II, and
98 analyzed the products by PAGE autoradiography (Fig. 2d). The SagB-SpdC cleavage
99 products shifted to higher molecular weight bands, showing they were competent
100 substrates and implying the presence of a diphospholipid at the reducing end.
101 Furthermore, when we treated the cleavage products with the bacteriocin colicin M, which
102 removes the lipid, we observed that the cleavage products migrated more slowly by SDS-
103 PAGE (Fig. 2e; Supplementary Fig. 8-10).^{24,25} LC-MS analysis confirmed the presence of
104 a diphosphate on a peptidoglycan fragment having an odd number of sugars, consistent
105 with glucosaminidase cleavage to leave a terminal MurNAc (Supplementary Fig. 10).
106 Notably, SagB-SpdC's cleavage activity *in vitro* depended on the conserved catalytic
107 glutamate^{13,2613,2613,2513,25,20} in SagB (E155), but not on an SpdC residue conserved in
108 eukaryotic CAAX proteases and required for their proteolytic activity (Supplementary Fig.
109 11). Moreover, cellular phenotypes of the SagB catalytic mutant resemble a *sagB*
110 knockout, whereas SpdC mutants lacking putative catalytic residues resemble wild-type
111 (Supplementary Fig. 12)¹⁵. These findings show that SagB plays a catalytic role in
112 peptidoglycan cleavage while SpdC plays a noncatalytic role in controlling SagB. While
113 we cannot exclude the possibility that SpdC has a catalytic function, its known *in vitro* and
114 cellular phenotypes involve noncatalytic functions.

115 These results show that the SagB-SpdC complex satisfies criteria expected for a
116 peptidoglycan release factor. First, the complex yields products that contain a reducing-
117 end lipid; second, these products are capable of further elongation. SagB's known effect
118 on glycan strand length may also be due to its role as part of a release factor complex. If
119 so, we would expect the loss of SpdC to similarly affect glycan strand length. By
120 comparing glycan strands isolated from wild-type, Δ *sagB*, and Δ *spdC* cells, we found that
121 the short glycan strands characteristic of wild-type *S. aureus* are lost in both the Δ *sagB*
122 and Δ *spdC* mutants (Supplementary Fig. 13), showing that SpdC is also involved in
123 glycan strand length control in cells. We would also expect SagB-SpdC to act on newly
124 synthesized sections of peptidoglycan polymer that are not yet modified or crosslinked
125 into the matrix because both proteins are anchored in the membrane. Consistent with this
126 expectation, we observed a clear preference for cleavage of nascent, unmodified
127 peptidoglycan over peptidoglycan that contained teichoic acid modifications or crosslinks
128 (Supplementary Fig. 14 and 15). Our conclusion that SagB-SpdC acts early in the
129 peptidoglycan maturation pathway is supported by recent studies that used atomic force
130 microscopy to visualize SagB mutants¹⁴.

131 To understand how SpdC interacts with SagB to control cleavage of nascent
132 polymer, we solved the structure of SagB complexed with a truncated form of SpdC
133 (SpdC¹⁻²⁵⁶) that lacks the cytoplasmic C-terminal domain (Fig. 3a-c; Supplementary Fig.
134 17)¹⁵. Removal of this apparently unstructured domain did not affect formation of the
135 complex or change its *in vitro* activity, nor did it impact cellular phenotypes of SpdC
136 (Supplementary Fig. 11, 16, 17). We refer hereafter to this truncated complex simply as
137 SagB-SpdC. Our structure, obtained using lipidic cubic phase (LCP) crystallography²⁷,

138 resolves nearly all of SpdC, which contains 8 transmembrane helices linked by short
139 extracellular and cytoplasmic loops, as well as the transmembrane helix and
140 glucosaminidase domain of SagB (Fig. 3c).

141 SagB makes contacts to SpdC on both its extracellular face and in the membrane
142 (Fig. 3a-c). A helix and loop in SagB's glucosaminidase domain (residues 115 to 127) sit
143 over the edge of the SpdC helical bundle and make extensive hydrogen bonding and ionic
144 interactions with the surface-exposed loop between SpdC transmembrane helix 3 (TM3)
145 and TM4 (Fig. 3b). Adjacent to this interface, the top of the SagB transmembrane helix
146 also contacts the SpdC TM3-TM4 loop (Q33, Fig. 3b), and from there the SagB TM helix
147 maintains tight hydrophobic contacts with SpdC TM3 across the membrane (Fig. 3c, and
148 also see Supplementary Fig. 19). We found that the SagB TM helix is required to form
149 the complex: SpdC did not co-purify with soluble SagB and swapping the TM helix of
150 SagB with that of SagA greatly reduced stability of the complex (Supplementary Fig. 19).
151 However, the SagB TM helix is not sufficient for robust complexation with SpdC; when
152 we replaced the TM helix of SagA with that of SagB, they did not co-purify as a 1:1
153 complex (Supplementary Fig. 19). Taken together, our results show that the
154 transmembrane interactions are necessary to form a complex, but are not sufficient for
155 the activity displayed by SagB-SpdC.

156 We thought the contacts at the extracellular SagB-SpdC interface could affect
157 cleavage function and made mutations predicted to disrupt key interactions. SagA and
158 SagB share the same fold and are 53% similar (Supplementary Fig. 3), but the
159 extracellular residues in SagB that contact SpdC are not conserved in SagA. Replacing
160 these residues on the extracellular SagB helix that contacts SpdC with the corresponding
161 SagA residues (SagB^{115-SEVNQLKKG-123}) did not prevent complex formation, which may be
162 driven largely by the interactions between TM helices in the membrane; however, we
163 observed an erosion of product length control (Fig. 3d, lane 5). We identified a possible
164 salt bridge between SagB lysine 118 and SpdC aspartate 106 in the crystal structure (Fig.
165 3b), and found that replacing either of these amino acids with a residue having the
166 opposite charge also resulted in a product distribution more closely resembling that of
167 purified SagB alone (Fig. 3d, lane 4). These results suggested that the relative orientation
168 of SpdC and the SagB glucosaminidase domain is important for determining the product
169 distribution.

170 To test whether the interface conformation observed in the crystal structure is
171 critical for product length control, we generated disulfide-linked SagB-SpdC complexes
172 using the crystal structure as a guide. We mutated proximal interface residues in SagB
173 and SpdC to cysteines and purified the corresponding complexes (Supplementary Fig.
174 20a). Both SagB^{N115C}-SpdC^{S107C} and SagB^{K118C}-SpdC^{D106C} complexes formed disulfide
175 linkages as judged by SDS-PAGE analysis. Both disulfide-linked complexes produced an
176 altered distribution of lipid-linked peptidoglycan products compared to wild-type (Fig. 3e
177 and Supplementary Fig. 20), with a shift to longer products. By comparing the mobility of
178 the lipid-linked SagB-SpdC cleavage products to Lipid II and short oligomers, we
179 concluded that the cleavage products from the disulfide-bonded complexes have 9-13
180 sugars (n=4-6; Supplementary Fig. 20). In an analogous experiment, unlabeled
181 peptidoglycan oligomers were treated with wild-type or the disulfide-bonded complex,
182 followed by ColM treatment and then LC-MS analysis. Similar to PAGE autoradiography,
183 the predominant species were longer for the reaction with the disulfide-bonded complex

184 (Fig. 3e). These results show that restricting the orientation of the two proteins to that
185 present in the crystal structure results in tighter length control. Noting that the crystal
186 structure was obtained in a membrane-like environment, we infer that this orientation is
187 relevant to the mechanism of cleavage in cells.

188 Our results suggest a mechanism for how SagB-SpdC generates the observed
189 product lengths (Fig. 4). The structure of SpdC is similar to that of the CAAX protease
190 Rce1 (Supplementary Fig. 21), which cleaves prenylated proteins just after the modified
191 cysteine residue. The resemblance of SpdC to a CAAX protease suggests that SpdC may
192 bind part of the lipid pyrophosphate carrier of nascent peptidoglycan. SpdC contains a
193 cavity that opens to the membrane between TM1 and TM5, a possible site of prenyl chain
194 entry. A groove extends from this opening along the extracellular face of SpdC all the way
195 to the active site pocket of SagB. Several lines of evidence have established the
196 directionality of oligosaccharide binding for the family of glucosaminidases to which SagB
197 belongs²⁸, and this directionality is consistent with nascent peptidoglycan following the
198 groove such that the non-reducing end of the polymer exits toward the cell wall
199 (Supplementary Fig. 22). Consistent with our model, we found that the distribution of
200 nascent cleavage products was unchanged whether polymerase and SagB-SpdC were
201 added simultaneously or sequentially (Supplementary Fig. 23). These results imply that
202 cleavage occurred after polymer release from the polymerase, leaving the substrate lipid
203 tail accessible for SpdC to bind. The product lengths observed *in vitro* are in good
204 agreement with the lengths that would be predicted from the physical dimensions of the
205 complex if the polymer tracks along the grooves in SpdC and SagB (Fig. 4b). To
206 determine if SagB-SpdC activity depends on the presence of the lipid portion of oligomers,
207 we pre-treated peptidoglycan with ColM and incubated the mixture with SagB-SpdC. As
208 analyzed by PAGE autoradiography, SagB-SpdC activity is abrogated when oligomers
209 lack the lipid, consistent with a role for the lipid in interacting with the complex
210 (Supplementary Fig. 24). Obtaining a structure of SagB-SpdC bound to a lipid-linked
211 nascent oligomer is now a key goal.

212 SagB-SpdC is the first example of a release factor complex shown to cleave
213 nascent peptidoglycan from its membrane anchor, which would allow its full integration
214 into the cell wall. As *S. aureus* can survive without SagB-SpdC, we infer that other
215 peptidoglycan release factors exist, and some may also be membrane-anchored cell wall
216 hydrolase complexes. We note that this first structure and biochemical analysis of a
217 bacterial member of the CAAX protease family suggests that other CAAX protease
218 homologs, which are widespread in bacteria, may also act to scaffold membrane proteins
219 involved in cell envelope synthesis.

220
221

222 **Acknowledgements**

223 We thank Dr. Samir Moussa for his preliminary experiments investigating the roles of
224 SpdC and SagB. We also thank Dr. Andrew Kruse for helpful discussions on
225 crystallography. This work used NE-CAT beamlines (GM103403), a Pilatus detector
226 (RR029205), and an Eiger detector (OD021527) at the APS (DE-AC02-06CH11357).
227 This research was supported by GM076710 and U19 AI109764 to D.K. and S.W. and
228 T32GM007753 to J.E.P.

229 **Data availability**

230 Transposon sequencing data (BioProject accession number PRJNA573479) can be found
231 in the NCBI BioProject database.

232 **Author contributions**

233 S.W., K.S., T.W.O., and J.E.P. designed experiments and analyzed the data with input
234 from D.K. K.S. performed the biochemical experiments; K.S. and T.W.O. purified proteins
235 and performed crystallographic experiments; J.E.P. analyzed transposon sequencing
236 data, constructed *S. aureus* mutant strains, performed the spot dilutions, and performed
237 the glycan strand experiment; S.W., K.S., T.W.O., J.E.P., and D.K. wrote the manuscript
238 with input from all authors.

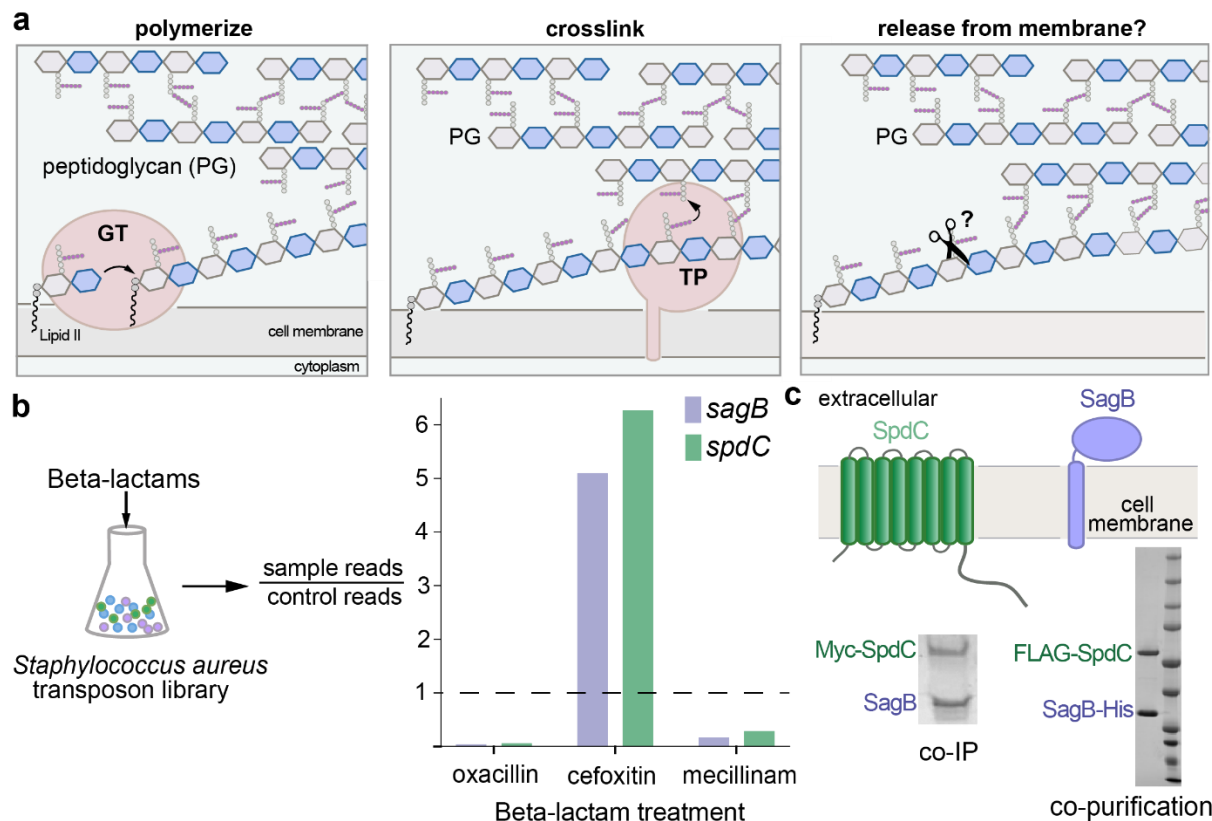
239 **Competing interests**

240 The authors declare no competing interests.

241

242

243



244

245 **Figure 1. The cell wall hydrolase SagB and the membrane protein SpdC form a complex.** **a**, Overview of the final
 246 steps in peptidoglycan assembly. Left panel: After translocation to the outer face of the cytoplasmic membrane, the
 247 peptidoglycan (PG) monomer Lipid II is polymerized into linear glycan strands by glycosyltransferases (GT). Middle
 248 panel: Transpeptidase domains (TPs) crosslink glycan strands into the cell wall. Right panel: The glycan strand must
 249 be released from the membrane through some type of cleavage process in order to be incorporated into the cell wall.
 250 **b**, A *Staphylococcus aureus* transposon library^{9,10} was treated with a panel of beta-lactams (oxacillin, cefoxitin,
 251 mecillinam) that have different selectivities for the four native *S. aureus* penicillin-binding proteins (PBPs)¹¹. Only two
 252 genes, *sagB* and *spdC*, displayed a response pattern in which transposon reads were depleted under oxacillin and
 253 mecillinam treatment but enriched under cefoxitin treatment. **c**, SagB is a membrane-anchored glucosaminidase^{12,13}
 254 and SpdC is an eight-pass membrane protein¹⁵. Myc-tagged SpdC was expressed in a $\Delta spdC$ *S. aureus* strain and co-
 255 immunoprecipitated from solubilized membranes. ("Co-IP", see also Supplementary Fig. 1). SagB was identified by LC-
 256 MS-MS analysis (Supplementary Table 1). Tandem affinity purification of SagB-His₆ and FLAG-SpdC from *E. coli*
 257 yielded a stable 1:1 complex ("co-purification", see also Supplementary Fig. 2).

258

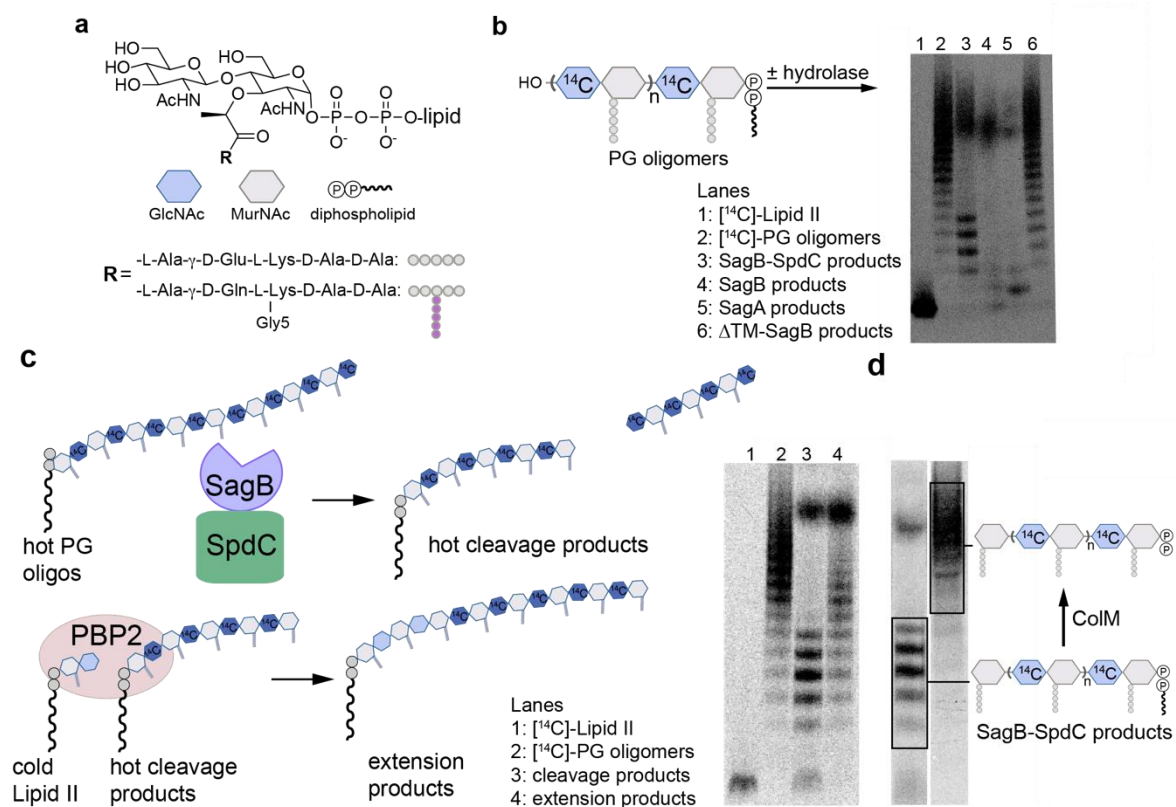
259

260

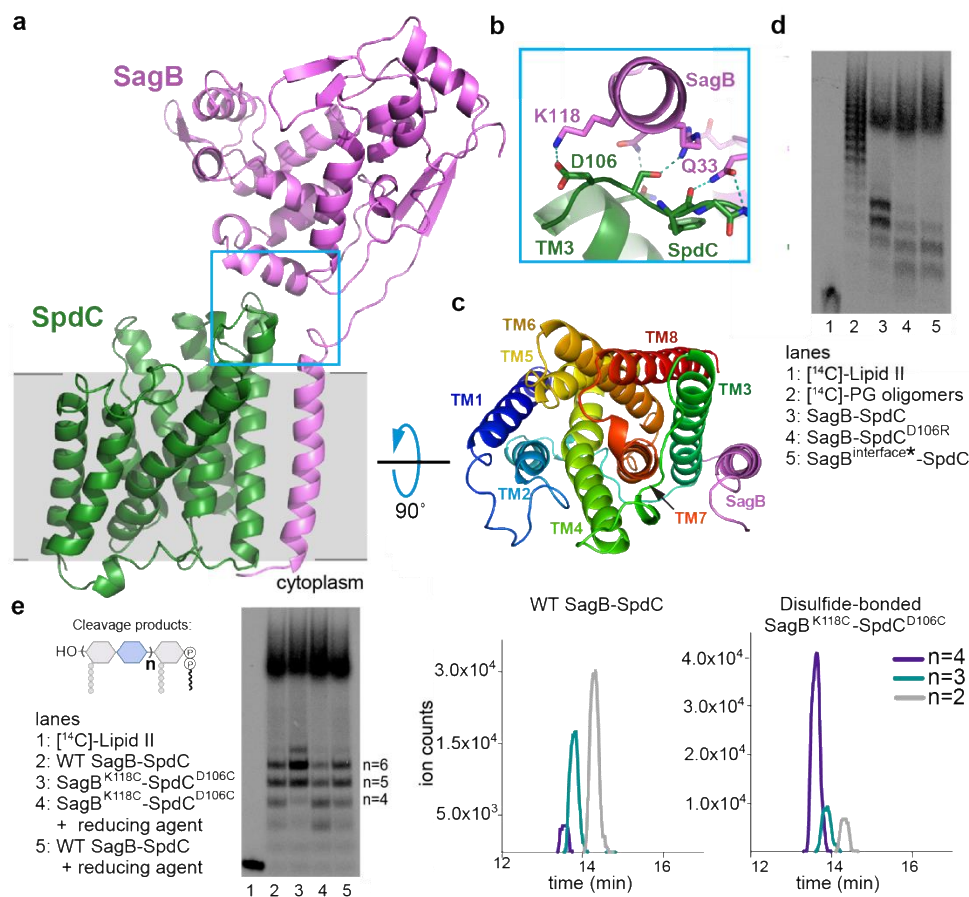
261

262

263

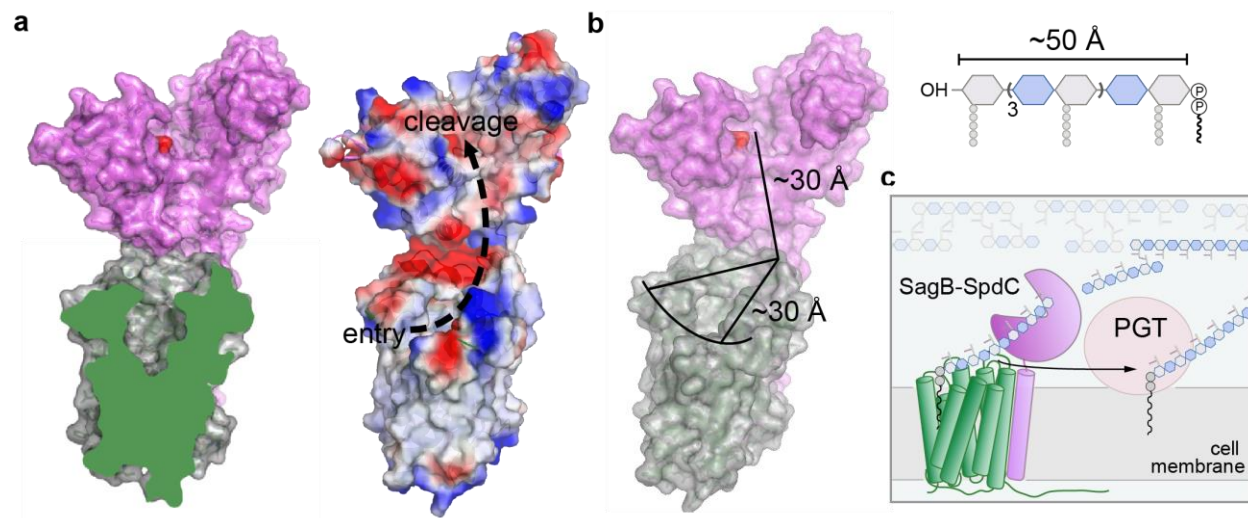


264
 265 **Figure 2. *In vitro* reconstitution shows that SagB-SpdC cleaves nascent peptidoglycan to short lipid-linked**
 266 **oligomers that can be elongated.** **a**, Chemical and cartoon representations of the synthetic Lipid II analog¹⁸ and
 267 native *S. aureus* Lipid II that were used to prepare peptidoglycan polymers in panels b-d. **b**, Radiolabeled peptidoglycan
 268 polymers were incubated with the SagB-SpdC complex, SagB alone, SagA, or SagB lacking its transmembrane helix.
 269 The signal towards the top of the autoradiograph in lanes 3-5 corresponds to short, lipid-free peptidoglycan fragments,
 270 but the distribution of lengths differs (Supplementary Fig. 6). SagB-SpdC also produces a short ladder of radiolabeled
 271 peptidoglycan fragments (see also Supplementary Fig. 5). **c**, Left: schematic of assay to determine whether SagB-
 272 SpdC product bands contained a lipid-anchor. Right: Radiolabeled SagB-SpdC products were incubated with
 273 unlabeled Lipid II and PBP2 and were extended to longer products. **d**, The bacteriocin colicin M (colM) de-lipidates
 274 Lipid II and peptidoglycan oligomers, but leaves the anomeric diphosphate (Supplementary Figs. 8, 9)^{23,24}.
 275 Incubation of SagB-SpdC products (lane 3) with ColM (lane 4) resulted in the complete disappearance of fast-migrating bands and
 276 the appearance of slower-migrating products. Product characterization by LC-MS confirmed the indicated structure
 277 (Supplementary Fig. 10). The faster migration of the SagB-SpdC products containing a lipid may be due to SDS binding
 278 to the lipid and increasing the net negative charge of these species.



279
 280
 281
 282
 283
 284
 285
 286
 287
 288
 289
 290
 291
 292
 293
 294
 295
 296

Figure 3. A 2.6 Å resolution crystal structure of the SagB-SpdC complex establishes that two interfaces are critical for its function. **a**, A cartoon representation of the SagB-SpdC crystal structure. The extracellular domains of both proteins interact (blue box); a helix at the bottom of the active site cleft of SagB (violet) contacts an extracellular loop between TM3 and TM4 of SpdC (green). The approximate location of the membrane is denoted in gray. **b**, Several hydrogen bonds and a salt-bridge form at the interface between the SagB helix and the SpdC loop. **c**, A view from the extracellular face of the transmembrane helices shows that SagB closely contacts TM3 of SpdC. SagB lacking its TM helix does not co-purify with SpdC (Supplementary Fig. 19). **d** and **e**, Radiolabeled peptidoglycan oligomers were incubated with SagB-SpdC or with constructs containing mutations designed to either disrupt or stabilize the extracellular interface between SagB and SpdC. **d**, SagB^{interface*} denotes SagB^{N115S, K118N, R119Q, V122D, D123G, L127E}, in which SagB residues at the interface were switched to the corresponding SagA residues. **e**, A variant of SagB-SpdC with two cysteine-substituted residues, SagB^{K118C}-SpdC^{D106C}, was purified as the disulfide-linked complex (Supplementary Fig 20). Activity of the oxidized complex (lane 3) was compared to the activity of SagB^{K118C}-SpdC^{D106C} incubated with reducing agent (lane 4), and to wild-type SagB-SpdC without and with reducing agent (lanes 2 and 5). Unlabeled cleavage products were also treated with ColM and analyzed using LC-MS analysis. Extracted ion chromatogram (EIC) traces are shown for both wild-type SagB-SpdC and SagB^{K118C}-SpdC^{D106C} reactions, and further confirm that longer oligosaccharide products are preferred for a disulfide-restricted complex. Notably, short oligosaccharides ionize better relative to longer oligosaccharides.



297

298 **Figure 4. SagB-SpdC is a peptidoglycan release factor that cleaves at a defined length from the reducing end**
299 **to allow strands to be fully incorporated into the cell wall.** **a**, A cross-section of SpdC shows a groove that extends
300 from the membrane and into the SagB catalytic groove (also see Supplementary Fig. 21d). As depicted by electrostatic
301 surface potential, SpdC provides a path for a glycan strand that extends from an “entry” point in the membrane and into
302 the “cleavage” site as denoted by the catalytic glutamate (red). **b**, Measuring the distance along this path provides
303 approximately equivalent lengths required for binding a glycan strand that represents the average lipid-linked product
304 lengths observed for the SagB-SpdC complex. **c**, Scheme depicting the proposed mode by which SagB-SpdC could
305 act as peptidoglycan release factor. To prevent wasteful release of lipid-free peptidoglycan fragments, SagB-SpdC
306 cleaves short strands that are being or have been crosslinked into the cell wall matrix; lipid-linked peptidoglycan
307 products can be further elongated by peptidoglycan polymerases (PGTs).
308

309

310

311

312

313

314

315

316

317

318

319

320

321

322

323

324

325

326

327

328

329

330
331
332
333
334
335
336
337
338
339
340
341
342
343
344
345
346
347
348
349
350
351
352
353
354
355
356
357
358
359
360
361
362
363
364
365
366
367
368
369
370
371
372
373
374
375
376
377
378
379
380
381
382

References:

- 1 Silhavy, T. J., Kahne, D. & Walker, S. The bacterial cell envelope. *Cold Spring Harb. Perspect. Biol.* **2**, a000414, doi:10.1101/cshperspect.a000414 (2010).
- 2 Vollmer, W., Blanot, D. & de Pedro, M. A. Peptidoglycan structure and architecture. *FEMS Microbiol. Rev.* **32**, 149-167, doi:10.1111/j.1574-6976.2007.00094.x (2008).
- 3 Meeske, A. J. *et al.* SEDS proteins are a widespread family of bacterial cell wall polymerases. *Nature* **537**, 634-638, doi:10.1038/nature19331 (2016).
- 4 Taguchi, A. *et al.* FtsW is a peptidoglycan polymerase that is functional only in complex with its cognate penicillin-binding protein. *Nat. Microbiol.* **4**, 587-594, doi:10.1038/s41564-018-0345-x (2019).
- 5 Sham, L. T. *et al.* Bacterial cell wall. MurJ is the flippase of lipid-linked precursors for peptidoglycan biogenesis. *Science* **345**, 220-222, doi:10.1126/science.1254522 (2014).
- 6 Ruiz, N. Bioinformatics identification of MurJ (MviN) as the peptidoglycan lipid II flippase in *Escherichia coli*. *Proc. Natl. Acad. Sci. USA* **105**, 15553-15557, doi:10.1073/pnas.0808352105 (2008).
- 7 Sauvage, E., Kerff, F., Terrak, M., Ayala, J. A. & Charlier, P. The penicillin-binding proteins: structure and role in peptidoglycan biosynthesis. *FEMS Microbiol. Rev.* **32**, 234-258, doi:10.1111/j.1574-6976.2008.00105.x (2008).
- 8 Yunck, R., Cho, H. & Bernhardt, T. G. Identification of MltG as a potential terminase for peptidoglycan polymerization in bacteria. *Mol. Microbiol.* **99**, 700-718, doi:10.1111/mmi.13258 (2016).
- 9 Santiago, M. *et al.* Genome-wide mutant profiling predicts the mechanism of a Lipid II binding antibiotic. *Nat. Chem. Biol.* **14**, 601-608, doi:10.1038/s41589-018-0041-4 (2018).
- 10 Santiago, M. *et al.* A new platform for ultra-high density *Staphylococcus aureus* transposon libraries. *BMC Genomics* **16**, 252, doi:10.1186/s12864-015-1361-3 (2015).
- 11 Georgopapadakou, N. H., Smith, S. A. & Bonner, D. P. Penicillin-binding proteins in a *Staphylococcus aureus* strain resistant to specific beta-lactam antibiotics. *Antimicrob. Agents Chemother.* **22**, 172-175, doi:10.1128/aac.22.1.172 (1982).
- 12 Wheeler, R. *et al.* Bacterial Cell Enlargement Requires Control of Cell Wall Stiffness Mediated by Peptidoglycan Hydrolases. *MBio* **6**, e00660, doi:10.1128/mBio.00660-15 (2015).
- 13 Chan, Y. G., Frankel, M. B., Missiakas, D. & Schneewind, O. SagB Glucosaminidase Is a Determinant of *Staphylococcus aureus* Glycan Chain Length, Antibiotic Susceptibility, and Protein Secretion. *J. Bacteriol.* **198**, 1123-1136, doi:10.1128/JB.00983-15 (2016).
- 14 Pasquina-Lemonche, L. *et al.* The architecture of the Gram-positive bacterial cell wall. *Nature*, doi:10.1038/s41586-020-2236-6 (2020).
- 15 Grundling, A., Missiakas, D. M. & Schneewind, O. *Staphylococcus aureus* mutants with increased lysostaphin resistance. *J. Bacteriol.* **188**, 6286-6297, doi:10.1128/JB.00457-06 (2006).
- 16 Poupel, O., Proux, C., Jagla, B., Msadek, T. & Dubrac, S. SpdC, a novel virulence factor, controls histidine kinase activity in *Staphylococcus aureus*. *PLoS. Pathog.* **14**, e1006917, doi:10.1371/journal.ppat.1006917 (2018).
- 17 Schaefer, K., Matano, L. M., Qiao, Y., Kahne, D. & Walker, S. In vitro reconstitution demonstrates the cell wall ligase activity of LCP proteins. *Nat. Chem. Biol.* **13**, 396-401, doi:10.1038/nchembio.2302 (2017).
- 18 Ye, X. Y. *et al.* Better substrates for bacterial transglycosylases. *J. Am. Chem. Soc.* **123**, 3155-3156, doi:10.1021/ja010028q (2001).
- 19 Qiao, Y. *et al.* Lipid II overproduction allows direct assay of transpeptidase inhibition by beta-lactams. *Nat. Chem. Biol.* **13**, 793-798, doi:10.1038/nchembio.2388 (2017).
- 20 Pintar, S., Borisek, J., Usenik, A., Perdih, A. & Turk, D. Domain sliding of two *Staphylococcus aureus* N-acetylglucosaminidases enables their substrate-binding prior to its catalysis. *Commun. Biol.* **3**, 178, doi:10.1038/s42003-020-0911-7 (2020).

- 383 21 Perlstein, D. L., Zhang, Y., Wang, T. S., Kahne, D. E. & Walker, S. The direction of glycan chain
384 elongation by peptidoglycan glycosyltransferases. *J. Am. Chem. Soc.* **129**, 12674-12675,
385 doi:10.1021/ja075965y (2007).
- 386 22 Wang, T. S. *et al.* Primer preactivation of peptidoglycan polymerases. *J. Am. Chem. Soc.* **133**,
387 8528-8530, doi:10.1021/ja2028712 (2011).
- 388 23 Welsh, M. A., Schaefer, K., Taguchi, A., Kahne, D. & Walker, S. The direction of chain growth and
389 substrate preferences of SEDS-family peptidoglycan glycosyltransferases. *J. Am. Chem. Soc.*,
390 doi:10.1021/jacs.9b06358 (2019).
- 391 24 El Ghachi, M. *et al.* Colicin M exerts its bacteriolytic effect via enzymatic degradation of
392 undecaprenyl phosphate-linked peptidoglycan precursors. *J. Biol. Chem.* **281**, 22761-22772,
393 doi:10.1074/jbc.M602834200 (2006).
- 394 25 Touze, T. *et al.* Colicin M, a peptidoglycan lipid-II-degrading enzyme: potential use for antibacterial
395 means? *Biochem. Soc. Trans.* **40**, 1522-1527, doi:10.1042/BST20120189 (2012).
- 396 26 Alcorlo, M., Martinez-Caballero, S., Molina, R. & Hermoso, J. A. Carbohydrate recognition and lysis
397 by bacterial peptidoglycan hydrolases. *Curr. Opin. Struct. Biol.* **44**, 87-100,
398 doi:10.1016/j.sbi.2017.01.001 (2017).
- 399 27 Caffrey, M. & Cherezov, V. Crystallizing membrane proteins using lipidic mesophases. *Nat. Protoc.*
400 **4**, 706-731, doi:10.1038/nprot.2009.31 (2009).
- 401 28 Mihelic, M. *et al.* The mechanism behind the selection of two different cleavage sites in NAG-NAM
402 polymers. *IUCrJ* **4**, 185-198, doi:10.1107/S2052252517000367 (2017).
- 403
404

405 **Methods and Materials**

406 **Materials**

407
408
409 All reagents and chemicals were purchased from Sigma-Aldrich unless indicated
410 otherwise. Lysostaphin was purchased from Ambicin. *Staphylococcus aureus* was grown
411 in tryptic soy broth (TSB) with aeration or on TSB with 1.5% agar at 30 or 37°C. Antibiotics
412 were used at the following concentrations for *S. aureus* strains: kanamycin (50 µg/mL),
413 neomycin (50 µg/mL), tetracycline (3 µg/mL), chloramphenicol (10 µg/mL), and
414 erythromycin (10 µg/mL). NovaBlue (DE3) *Escherichia coli* (*E. coli*) strains were grown in
415 Lysogeny broth (LB). BL21(DE3) *E. coli* strains were grown in terrific broth at
416 temperatures between 18°C and 37°C as described below. Native Lipid II was extracted
417 from *Staphylococcus aureus* as previously described¹⁹. Synthetic Lipid II was prepared
418 as previously described¹⁸. The radiolabeled wall teichoic acid (WTA) precursor, [¹⁴C]-
419 LII_A^{WTA}, was prepared as previously reported¹⁷. Fmoc-Biotin-D-Lysine (BDL) was used
420 to prepare BDL²⁹. PBP2^{S398G}, SgtB^{Y181D}, EfPBPX, and TagT were expressed and purified

421 as described in previous methods^{19,30-32}. Colicin M was expressed and purified as
422 previously described⁵. LytA was expressed and purified as previously described³³.

423 **Methods**

424 **Beta-lactam treatment and sequencing of a methicillin-resistant *Staphylococcus*** 425 ***aureus* transposon library**

426
427 We created a high-density transposon library in *S. aureus* USA300 by phage-
428 based transposition as previously described^{9,10,34}. The transposon library was treated with
429 beta-lactams (8 µg mL⁻¹ for mecillinam, 0.4 µg mL⁻¹ for cefoxitin, and 0.1 µg mL⁻¹ for
430 oxacillin) at 37°C. A low concentration of oxacillin was chosen to identify factors important
431 for beta lactam resistance. For mecillinam and cefoxitin, the concentrations were chosen
432 such that only one PBP should be significantly inhibited in each condition. For mecillinam,
433 the concentration was that at which the treated cells phenocopied a *pbp3* mutant at 43
434 °C. For cefoxitin, the concentration was that which sensitized cells to oxacillin to the same
435 degree as a *pbp4* mutant. Cultures were shaken until A₂₈₀=1-2.0. Cells were spun down,
436 and DNA was isolated in preparation for Tn-Seq as previously described. Using reported
437 methods^{9,10}, genes significantly enriched and depleted under cefoxitin, mecillinam, or
438 oxacillin conditions were identified using a two-sided Mann-Whitney U test corrected for
439 multiple hypothesis testing using the Benjamini-Hochberg method. A gene was
440 considered to be enriched if the treated:control read ratio was greater than five and
441 depleted if the treated:control read ratio was less than 0.1. For mecillinam, the cut-off for
442 depletion was loosened to 0.3, as mecillinam was moderately selective. Scripts for this
443 analysis can be found at <https://github.com/SuzanneWalkerLab/TnSeqMOAPrediction>.

445 **Plasmid construction for *S. aureus* strains**

446
447 *pKFC_spdC_kan*

448
449 The kan^R marker (primers SM45 and SM46) and the 1-kb sequences upstream
450 (primers SM43 and SM44) and downstream (primers SM47 and SM48) of the *spdC* open
451 reading frame were amplified by PCR and stitched together by overlap PCR. The resulting
452 fragment was cloned between the BamHI and Sall restriction sites of pKFC.³⁵

453 *pKFC_spdC*

454 The 700-bp sequences upstream (primers SM1 and SM2) and downstream
455 (primers SM3 and SM4) of the *spdC* open reading frame were amplified by PCR and
456 stitched together by overlap PCR. The resulting fragment was cloned between the BamHI
457 and Sall restriction sites of pKFC.

458 *pJP47*

459 The pTarKO vector was linearized with primers F_pKTarO and R_pKTarO using
460 the plasmid pTD47³⁶ as a template. The 1-kb sequences upstream (primers
461 F_1kb+_sagB and R_1kb+_sagB) and downstream (F_1kb(-)_sagB and R_1kb(-)_sagB)
462 of the *sagB* open reading frame were amplified by PCR. Overlap PCR was performed to
463 assemble these fragments with the tet^R marker, and then the resulting fragment was
464 ligated into the plasmid backbone between the restriction sites BamHI and Sall. Then,
465 the tet^R marker (primers oJP51 and oJP52) and upper homology arm (primers oJP54 and
466 oJP33) were sequentially replaced by Takara Bio In-Fusion seamless cloning after
467 linearizing the plasmid with primers oJP49 and oJP50 and oJP53 and oTD145
468 respectively. The insert containing the *sagB* homology arms and tet^R marker was
469 amplified with primers oJP32 and oJP35 and cloned between the BamHI and Sall
470 restriction sites in pKFC. To exchange the tet^R marker for a kan^R marker, this plasmid
471 was linearized with primers oJP79 and oJP80. The linearized DNA was phosphorylated

472 at the 5' ends using T4 polynucleotide kinase, and the ends were ligated to produce
473 circular DNA. The kan^R marker (primers oTD73 and oTD74) was then cloned into the
474 plasmid at the XbaI restriction site. Finally the insert containing the *sagB* homology arms
475 and the kan^R marker was amplified with primers oJP32 and oJP35 and cut into the
476 pTarkO backbone between the BamHI and Sall restriction sites³⁷.

477 *pSM_spdC_myc*, *pJP17*, and *pJP42*

478 For pSM_spdC_myc and pJP42, the full or truncated *spdC* gene sequence with its
479 native ribosome-binding site (-17) was amplified from HG003 *S. aureus* genomic DNA
480 and an amino-terminal cMyc tag appended by PCR using primers SM165 and SM166 for
481 pSM_spdC_myc and primers oJP25 and oJP81 for pJP42. The fragments were then
482 cloned between the KpnI and BlnI restriction sites of pTP63.³⁸ For pJP17, the cMyc-*spdC*
483 fragment with the native ribosome binding site was amplified from pSM_spdC_myc using
484 primers oJP25 and oJP26 and cloned between the KpnI and BlnI restriction sites of
485 pTP63.

486 *pSM_spdC_his*

487 The *spdC* gene and native ribosome-binding site was amplified from HG003 *S.*
488 *aureus* genomic DNA and a carboxy-terminal hexa-histidine tag was appended by PCR
489 with primers SM124 and SM125. This fragment was cloned between the KpnI and BlnI
490 restriction sites of pTP63.

491 *pSM_spdC_E135A*, *pSM_spdC_R139A*, *pSM_spdC_H210A*

492 These three plasmids were constructed using QuikChange site-directed
493 mutagenesis with primers SM130 and SM131, SM132 and SM133, and SM134 and
494 SM135 respectively and *pSM_spdC_his* as a template.

495 *pJP15 and pJP19*

496 The *sagB* or *sagB E155A* gene sequence with a carboxy-terminal hexa-histidine tag was
497 amplified from *pspdC_sagB* or *pspdC_sagB^{E155A}* respectively and the native ribosome
498 binding site appended by PCR with primers oJP21 and oJP22. The fragments were
499 cloned between the KpnI and BlnI restriction sites in pTP63.

500 *pJP22*

501 A gBlock gene fragment was synthesized by IDT. The fragment was amplified with
502 primers oJP30 and oJP31 and cloned between the KpnI and BlnI restriction sites in
503 pTP63.

504

505 ***S. aureus* strain construction**

506

507 pKFC_*spdC*_kan and pKFC_*spdC* were used to construct SHM056 and SHM002
508 respectively using a previously published method³⁵. pJP47 was used to construct JP132
509 using a previously published method³⁷. The deletions, or in the case of SHM002 the
510 integrated plasmid before recombination, were transduced to HG003 *S. aureus*. The final
511 deletions were confirmed by colony PCR and sequencing. Phage transductions were
512 performed using a previously published protocol³⁹.

513 To construct JP012 and JP065, a phage lysate was prepared from SAUSA300 JE2
514 *sagB::Tn-erm^R* from the Nebraska library and used to transduce HG003 *S. aureus* and
515 SHM056 respectively.

516 To construct strains containing pTP63³⁸ constructs, the plasmids were first
517 electroporated into TD011, and transformants were selected on 10 µg/mL
518 chloramphenicol at 30°C. The pTP63 constructs were transduced from these

519 transformants into strain JP012 to produce strains JP051 and JP053 and into SHM056 to
520 produce SHM226, JP054, JP064, and JP128. For JP061, JP062, and JP063, the pTP63
521 constructs were first transduced into SHM002, and from there transduced into SHM056.

522 **Co-immunoprecipitation with Myc-tagged SpdC in *Staphylococcus aureus***

523
524 This protocol was adapted from previously published protocols⁴⁰. An overnight
525 culture of SHM226 was diluted 1:100 into 1 L of TSB. The culture was grown at 37°C with
526 shaking at 200 r.p.m. until $A_{600\text{nm}} = 0.6$ and then 0.2 μM anhydrotetracycline was added
527 to induce plasmid expression. After a 3 h induction, cells were pelleted at 5000xg, 15
528 minutes, 4°C. Cell pellets were then resuspended in lysis buffer (1X PBS (pH 7.4), 20 μg
529 mL^{-1} DNase and RNase, 10 μg mL^{-1} lysostaphin, 5 mM MgCl_2) and incubated at 37°C for
530 1 h. In samples treated with a chemical crosslinker, 0.5 mM DSP was added to the mixture
531 for 1 h and then quenched with 20 mM Tris (pH 7.5). After cooling on ice, cells were lysed
532 with a French press two times at 20,000 psi on a high ration setting. Unbroken cells were
533 then removed by centrifugation at 10,000xg, 4°C, 15 min. Membranes were pelleted by
534 ultracentrifugation at 100,000xg, 4°C for 60 minutes in a Beckman 45Ti rotor. For
535 solubilization, membrane pellets were resuspended in buffer B (1X PBS (7.4), 500 mM
536 NaCl, 1% Triton X-100). Cell membranes were then rocked at 4°C overnight before
537 insoluble cell debris was removed by ultracentrifugation at 100,000xg, 4°C, 30 minutes.
538 Equilibrated magnetic anti-Myc beads (Clontech, Catalog #635699) were then added to
539 the solubilized membranes and rocked at 4°C overnight. Equilibrated beads were then
540 washed three times with wash buffer (1X PBS pH 7.4, 200 mM NaCl, 1% Triton X-100).
541 Protein was eluted with elution buffer provided in the Myc Immunoprecipitation kit
542 (Clontech, Catalog # 635698). Elution buffer was then neutralized with 1 N NaOH before

543 running on a 4-20% SDS-PAGE gel. Protein bands were prepared for LC-MS-MS
544 analysis, adapted from previous protocols. Protein bands were excised from the gel and
545 stored in deionized H₂O prior to submission for LC-MS-MS analysis at the Taplin Mass
546 Spectrometry Facility, Harvard Medical School.

547 **Spot dilution assay**

548 Overnight cultures were diluted 1:100 into 3 mL TSB and grown at 30 °C with
549 aeration until mid-log phase. Cultures were then diluted to OD₆₀₀ = 0.5. Five 10-fold serial
550 dilutions of the resulting cultures were prepared for each strain, and 5 µL of each dilution
551 was spotted on TSA plates with or without 0.4 µM anhydrotetracycline inducer and, where
552 indicated, 0.8 µg/mL tunicamycin or 1 µg/mL lysostaphin. Plates were imaged after
553 approximately 16 hours of incubation at 30 °C. Strains HG003 wild-type, SHM056, JP012,
554 JP051, JP053, JP054, JP061, JP062, JP063, JP064, JP065, and JP128 were used for
555 these assays.

556 **Cloning, expression, and purification of *S. aureus* glucosaminidases and SpdC** 557 **variants**

558 **Cloning of *S. aureus* glucosaminidases and SpdC**

559 Genes encoding SagA (SAV2307), SagB (SAOUHSC_01895), and SpdC
560 (SAOUHSC_02611) were amplified by PCR from *Staphylococcus aureus* strain NCTC
561 8325 genomic DNA. For co-expression, SagB and SpdC were cloned into a pDUET
562 containing an amino-terminal SUMO-fusion followed by a Flag epitope tag and a carboxy-
563 terminal hexa-histidine tag in another site. SagB and SpdC were amplified using
564 F_SagB/R_SagB and F_SpdC/R_SpdC, and ligated into the pDUET, using primers
565 F_DUET_SagB/R_DUET_SagB and F_DUET_FLAG_SpdC/R_DUET_FLAG_SpdC in
566 two steps using Gibson assembly (New England Biolabs, # E2611L). Similar methods
567
568

569 were used for SagA and SpdC co-purification. Oligonucleotide primers were purchased
570 from Eton Bio.

571 **Expression and co-purification of full-length, wild-type *S. aureus* SagB and SpdC**

572
573 For co-expression of *S. aureus* SagB and SpdC, overnight cultures of BL21(DE3)
574 *E. coli* containing pDUET-SUMO-FLAG-SpdC and SagB-His₆ and an arabinose-inducible
575 Ulp1 protease plasmid³ (pAM174) were diluted 1:100 into terrific broth supplemented with
576 50 µg ml⁻¹ carbenicillin and 35 µg ml⁻¹ chloramphenicol. Cultures were grown at 37°C with
577 shaking at 200 r.p.m. until A_{600nm} = 0.6 and then shifted to 18°C. At an A_{600nm} = 1.0, protein
578 expression was induced by addition of 0.5 mM isopropyl-β-D-thiogalactoside (IPTG) for
579 SagB and SpdC expression, and 0.2% arabinose for Ulp1 expression. After a 18 h
580 expression, cells were collected by centrifugation and resuspended in buffer containing
581 50 mM Tris-HCl (pH 7.4), 300 mM NaCl, 1 mM phenylmethylsulfonyl fluoride (PMSF), 1
582 cOmplete protease inhibitor table (Sigma-Aldrich), 50 µg/ml DNase 1. Resuspended cells
583 were lysed by a 4x passage through an Emulsiflex C3 homogenizer (Avestin) at 15,000
584 p.s.i. Lysed cells were separated from unbroken cells by centrifugation at 12,000g, 4°C
585 for 10 minutes. Membranes were pelleted by ultracentrifugation at 100,000g, 4°C for 60
586 minutes in a Beckman 45Ti rotor. For solubilization, membrane pellets were resuspended
587 in buffer B (50 mM Tris-HCl (7.4), 300 mM NaCl, 10% glycerol), homogenized using an
588 IKA T18 UltraTurrax, and then supplemented with 1% w/v dodecyl-maltoside (DDM;
589 Anatrace). Cell membranes were rocked at 4°C for 1 hour before insoluble cell debris was
590 removed by ultracentrifugation at 100,000xg, 4°C, 30 minutes. Equilibrated Ni-NTA
591 agarose (equilibrated with buffer B supplemented with 10 mM imidazole; Qiagen) was
592 resuspended with solubilized membranes and rocked at 4°C for 1 hour before gravity flow

593 through a column. Following flow-through, resin was washed with 20 column volumes (cv)
594 of buffer B supplemented with 10 mM imidazole and 0.05% DDM and then 20 cv of buffer
595 B with 30 mM imidazole and 0.05% DDM. Protein was eluted with 4 cv buffer B with 200
596 mM imidazole, 0.05% DDM, and 2 mM CaCl₂. Elution fractions were then loaded onto a
597 4 mL M1-anti-Flag antibody affinity resin using gravity flow twice. The resin was then
598 washed with 100 ml buffer containing 50 mM HEPES (pH 7.5), 300 mM NaCl, 10%
599 glycerol, 0.05% DDM, and 2 mM CaCl₂. Protein was eluted in 20 mM HEPES (pH 7.5),
600 500 mM NaCl, 20% glycerol, 0.1% DDM supplemented with 5 mM EDTA and 0.2 mg ml⁻¹
601 ¹ Flag peptide (Genescript). SagB-SpdC was concentrated using a 50 MWCO
602 concentrator (Amicon) and further purified by size exclusion chromatography on a
603 Sephadex S200 Increase 10/300 GL (GE Healthcare) in buffer (for biochemical reactions,
604 buffer contained 50 mM Tris-HCl (7.4), 300 mM NaCl, 10% glycerol, 0.1% DDM; for
605 crystallography, buffer contained 50 mM Tris-HCl (7.4), 300 mM NaCl, 3% glycerol,
606 0.02% DDM). For biochemical reconstitutions, SagB-SpdC was concentrated into
607 approximately 2 mg ml⁻¹ aliquots, flash-frozen with liquid nitrogen, and stored at -80°C.
608 The attempted purification of SagA-SpdC used a similar protocol, with the expression
609 plasmid containing SagA-His₆ in place of SagB.

610 **Expression and purification of *S. aureus* individual glucosaminidases and SpdC**

611 Individual SagB-His₆, SagA-His₆, and FLAG-SpdC were expressed and purified in
612 a similar manner as described above with the following modifications. Overnight culture
613 of BL21(DE3) *E. coli* containing the plasmid with SagA, SagB, or SpdC was diluted 1:100
614 in terrific broth supplemented with 0.1% glucose and 50 µg ml⁻¹ carbenicillin. Growth
615 conditions and initial purification steps were similar to as described above, with the
616 exception of using a Ni_NTA resin to bind and purify individual hydrolases and the M1-

617 anti-FLAG resin to bind and purify SpdC. After elution from respective resin, protein was
618 concentrated using a 30 MWCO concentrator and further purified using a Sephadex 200
619 10/300 GL column using buffer containing 50 mM Tris-HCl (pH 7.4), 300 mM NaCl, 0.1%
620 DDM, 10% glycerol.

621 For the soluble SagB construct, protein was expressed and purified in the same
622 manner with slight modifications. Overnight cultures of BL21 (DE3) *E. coli* containing a
623 pET_28(b)+ with SagB lacking its transmembrane helix (32-284 aa) was diluted 1:100 in
624 LB. Cells were grown at 37°C at 200 r.p.m. until $A_{600nm}=0.4$ and then cooled to 18°C; at
625 $A_{600nm}=0.6$, protein expression was induced with 0.5 mM IPTG. After 18 hr expression,
626 cells were collected by centrifugation and lysed as described above. After lysis, unbroken
627 cell debris was removed by centrifugation at 12,000g, 4°C for 10 minutes. Supernatant
628 was further clarified by ultracentrifugation at 100,000g, 4°C for 30 minutes. Ni-NTA resin
629 was equilibrated with clarified supernatant for 1 hour, rocking at 4°C. Following flow-
630 through, resin was washed with 20 column volumes (cv) of buffer B supplemented with
631 10 mM imidazole and then 20 cv of buffer B with 30 mM imidazole. Protein was
632 concentrated using a 10 MWCO concentrator tube (Amicon) and then further purified
633 using size exclusion chromatography with Sephadex 75 10/300 GL and a buffer
634 containing 50 mM Tris-HCl (pH 7.4), 300 mM NaCl, 10% glycerol. Aliquots of
635 concentrated soluble SagB at approximately 2-4 mg ml⁻¹ were then flash-frozen with liquid
636 nitrogen and stored at -80°C.

637 **Expression and purification of *S. aureus* SagB with truncated SpdC (1-256 amino**
638 **acids)**

639 *S. aureus* SagB-SpdC (1-256 amino acids) was expressed and purified in the
640 same manner with slight modifications. Overnight cultures of BL21(DE3) *E. coli* containing

641 the pDUET with SUMO_Flag_SpdC (1-256 aa) and SagB-His₆, and an arabinose-
642 inducible Ulp1 protease plasmid (pAM174) were diluted 1:100 in terrific broth
643 supplemented with 0.1% glucose. Cultures were grown at 30°C with shaking at 200 r.p.m.
644 until A_{600nm} = 0.6 and then shifted to 24°C. At an A_{600nm} = 1.1, protein expression was
645 induced by addition of 0.5 mM isopropyl-β-D-thiogalactoside (IPTG) for SagB and SpdC
646 expression, and 0.2% arabinose for Ulp1 expression and grown for 16 h. Purification of
647 SagB-SpdC was similar to as described above.

648

649 **Expression and purification of *S. aureus* SagB-SpdC cysteine mutants**

650 The *S. aureus* SagB-SpdC cysteine mutants were expressed and purified in the
651 same manner with slight modifications. Overnight cultures of BL21(DE3) *E. coli* containing
652 the pDUET with SUMO_Flag_SpdC and SagB-His₆ with the cysteine mutants, and an
653 arabinose-inducible Ulp1 protease plasmid (pAM174) were diluted 1:100 in terrific broth
654 supplemented with 0.1% glucose. Cultures were grown at 25°C with shaking at 200 r.p.m
655 until A_{600nm} = 0.6 and then shifted to 20°C. At an A_{600nm} = 1.1, protein expression was
656 induced by addition of 0.5 mM isopropyl-β-D-thiogalactoside (IPTG) for SagB and SpdC
657 expression, and 0.2% arabinose for Ulp1 expression and grown for 16 hours. Purification
658 of SagB-SpdC was similar to as described above with the following modifications.
659 Pelleted cells were resuspended in 50 mM Tris-HCl (pH 7.4), 300 mM NaCl, 1 mM
660 phenylmethylsulfonyl fluoride (PMSF), 1 cOmplete protease inhibitor table (Sigma-
661 Aldrich), 50 µg/ml DNase 1. To facilitate disulfide formation, 0.3 mM CuSO₄ and 0.3 mM
662 1,10-phenanthroline were added to the mixture. The remaining purification steps followed
663 those described above.

664 **PAGE autoradiograph experiments with PG oligomers and *S. aureus* hydrolases**

665 The protocol for analyzing and preparing peptidoglycan oligomers was adapted
666 from similar methods previously reported^{17,41}. A PBP2 construct¹⁹ (59-716 amino acids,
667 1 μ M) was incubated with synthetic-[¹⁴C]-Lipid II analog¹⁸ (20 μ M in DMSO; specific
668 activity=300 μ Ci/ μ mol from UDP-[¹⁴C]-GlcNAc (American Radiolabeled Chemicals, Inc.)
669 in reaction buffer (50 mM MES (6.5), 100 mM CaCl₂) with 20% DMSO (v/v). After mixing
670 the Eppendorf tube by flicking and spinning down the reaction mixture, polymerization
671 proceeded at room temperature for 2 hours. To test oligomers prepared from SgtB*
672 (SgtB^{Y181D})³⁰, similar conditions were set up with 800 nM SgtB*. Proteins were removed
673 by precipitation by heating the reaction mixture at 95 °C for 10 minutes and then spinning
674 down the precipitated protein. The PG oligomers were then aliquoted into separate
675 Eppendorf tubes (10 μ l mixture for each reaction) and a hydrolase (SagA, SagB, SagB-
676 SpdC, or the Δ TM-SagB; 3 μ M) was added. For reactions in which the individual
677 hydrolase was incubated with SpdC, the hydrolase SagA or SagB (3 μ M) were added to
678 SpdC (3 μ M) for 1 hour on ice before addition to the PG mixture. After overnight
679 incubation, the reaction was quenched with heat inactivation (95 °C for 10 minutes) and
680 the reactions were dried completely using a speed vacuum. Reactions were resuspended
681 in 10 μ l of SDS loading buffer and loaded onto a 10% acrylamide-Tris gel. The gel was
682 run at 30 mA for 5 h at 4°C; an anode buffer consisted of 100 mM Tris (pH 8.8) and
683 cathode buffer consisted of 100 mM Tris, 100 mM tricine (pH 8.25), 0.1% SDS⁴¹. Gels
684 were dried on filter paper (19 x 18.5 cm; Biorad) and then exposed to a phosphor screen
685 for at least 24 h. Phosphor screens were imaged using an Azure Sapphire Biomolecular
686 Imager (Azure biosystems). Images were further analyzed using ImageJ.

687 Reactions to test hydrolase activities with concurrent PBP2 transglycosylase
688 activity were set up and analyzed in a similar manner with some modifications. A reaction
689 mixture was prepared with synthetic-[¹⁴C]-Lipid II analog¹⁸ (20 μM in DMSO; specific
690 activity=300 μCi μmol⁻¹ from UDP-[¹⁴C]-GlcNAc (American Radiolabeled Chemicals,
691 Inc.), reaction buffer (50 mM MES (6.5), 100 mM CaCl₂), 20% DMSO (v/v). PBP2 (59-
692 716 amino acids; 5 μM) and the hydrolase (SagA, SagB, SagB-SpdC; 3 μM) was then
693 added). Similar methods were used to test the activities of interface mutants of SagB-
694 SpdC. To test the activities of disulfide-linked SagB-SpdC complexes, protein under
695 reducing conditions were treated with 5 mM DTT on ice for 30 minutes before the addition
696 to the reaction mixture that included the addition of 5 mM DTT. After overnight incubation,
697 the reaction was quenched with heat inactivation (95 °C for 10 minutes) and the reactions
698 were dried completely using a speed vacuum. Reactions were resuspended in 10 μl of
699 2x SDS loading buffer and loaded onto a 10% acrylamide-Tris gel. The gel was run and
700 analyzed as described above.

701 Testing hydrolase activities with wall-teichoic acid labeled peptidoglycan oligomers
702 was adapted from similar methods previously reported³⁶. Peptidoglycan oligomers were
703 prepared as described above although with unlabeled, synthetic-Lipid II (20 μM). After
704 precipitation to remove the PGT, a portion of the mixture was incubated with TagT (1 μM)
705 and [¹⁴C]-LII^A^{WTA} (8 μM) for four hours at room temperature. The TagT ligase was then
706 heat inactivated, precipitated, and removed from the reaction mixture. The resulting wall
707 teichoic acid-labeled oligomers were then incubated with SagB (3 μM), SagB-SpdC (3
708 μM), or mutanolysin (2.5 U ml⁻¹). The remaining portion of unlabeled PG oligomers was
709 also incubated with the SagB-SpdC complex (3 μM). After an overnight incubation at room

710 temperature, the reaction was quenched with heat inactivation (95 °C for 10 minutes). To
711 test TagT ligation after SagB-SpdC incubation, TagT (1 μM) and [¹⁴C]-LII^{WTA} (8 μM) was
712 added to the respective reaction for four additional hours. Reactions were dried
713 completely using a speed vacuum and the mixture was re-dissolved in 10 μl of 2x SDS
714 loading buffer and loaded onto a 10% acrylamide-Tris gel. The gel was run and analyzed
715 as described above.

716 **Western blot analysis of hydrolase activities with peptidoglycan oligomers**
717 **prepared from *S. aureus* Lipid II**

718 The protocol for detecting peptidoglycan oligomers prepared from extracted *S.*
719 *aureus* Lipid II was adopted from similar methods previously reported^{19,23,29}. To generate
720 uncrosslinked PG oligomers, *S. aureus* Lipid II (10 μM) was added to reaction buffer (50
721 mM MES (6.5), 10 mM CaCl₂), 20% DMSO (v/v) and the transpeptidase inactive construct
722 PBP2^{S398G} (5 μM) was added to the reaction. To test ongoing hydrolase and polymerase
723 activity, the reaction mixture was aliquoted into separate tubes and the respective
724 glucosaminidase was also added (SagA, SagB, or SagB-SpdC; 3 μM). For a mutanolysin-
725 digest reaction, 2.5 U ml⁻¹ of mutanolysin (Sigma-Aldrich) was added⁴². If testing
726 hydrolase activity with pre-assembled PG oligomers, PBP2^{S398G} was precipitated after
727 heat inactivation at 95°C. PG oligomers were aliquoted into separate 10 μl reactions, and
728 the hydrolase was added as described above. Reactions were inactivated at 95°C for 10
729 minutes. To label uncrosslinked PG oligomers, BDL (4 mM in H₂O) and *E. faecalis* PBPX³¹
730 (20 μM) was added to the reaction mixtures. After a 1 h incubation at room temperature,
731 2x loading buffer was added to quench the reactions. To generate crosslinked PG, *S.*
732 *aureus* Lipid II (10 μM) was added to reaction buffer (50 mM MES (6.5), 10 mM CaCl₂),
733 20% DMSO (v/v), BDL (4 mM), and a wild type PBP2 construct (5 μM). After the addition

734 of PBP2, the respective glucosaminidase was also added (SagB or SagB-SpdC; 3 μ M)
735 and the reactions were incubated at room temperature for 5 hours. Reactions were split
736 into two aliquots after heat inactivation at 95°C, and lysostaphin (100 μ g ml⁻¹) was added
737 to one aliquot and then incubated at 37°C for 2 hours. 2x loading dye was added to each
738 reaction, and these mixtures were loaded onto a 4-20% polyacrylamide gel which ran at
739 175 V for 1 h. The gel was transferred to PVDF membrane (Biorad) at 10 mV for 1 h. After
740 incubating with starting block (Thermo Scientific, catalog number #37578), the membrane
741 was rocked with HRP-streptavidin (1:5000) in TBS-T and then washed repetitively. The
742 membrane was imaged using the chemiluminescence function on an Azure imager
743 (Azure biosystems). Images were further analyzed using ImageJ.

744

745 **LC-MS method for detecting digest products of *S. aureus* glucosaminidases and** 746 **mutanolysin**

747 The cleaved muropeptide products of glucosaminidase reactions (SagA, SagB,
748 SagB-SpdC) were analyzed by adopting a previously reported LC-MS method for
749 detecting mutanolysin-digested products⁴². Hydrolase reactions were prepared using
750 synthetic Lipid II (20 μ M), reaction buffer (50 mM MES (6.5), 10 mM CaCl₂), 20% DMSO
751 (v/v), PBP2S398 (5 μ M), and then the respective hydrolase (SagA, SagB, SagB-SpdC, 3
752 μ M) in a total volume of 50 μ l. A control mutanolysin reaction was likewise set-up with 5
753 U ml⁻¹ mutanolysin. After an overnight incubation, sodium borohydride (10 mg ml⁻¹ in H₂O;
754 equal reaction volume) was added and incubated for 20 minutes at room temperature.
755 The reaction was quenched with the addition of 20% phosphoric acid which also adjusted
756 the pH to 3-4. Reactions were completely dried under a nitrogen stream and then
757 resuspended in H₂O. LC-MS analysis was conducted using an Agilent Technologies 1200

758 series HPLC in line with an Agilent 6210 TOF mass spectrometer with electrospray
759 ionization (ESI) and operating in positive mode. Muropeptide cleavage products were
760 separated using a Waters Symmetry Shield RP18 column (5 μm , 3.9 x 150 mM) with a
761 matching guard column and the following method: 0.4 mL min^{-1} solvent A (water/0.1%
762 formic acid) for 5 minutes followed by a linear gradient of 0 to 40% solvent B
763 (acetonitrile/0.1% formic acid) over 25 min. Mass spectrometry data was analyzed using
764 Agilent MassHunter Workstation Qualitative Analysis software version B.06.00 and Prism
765 7.0b.

766 **LC-MS method for detecting lipid-linked PG oligomers**

767 To character lipid-linked cleavage products, we adapted previously published
768 methods²³. Peptidoglycan oligomers were prepared by incubating Lipid II (40 μM) with
769 PBP2^{S398G} (5 μM) in 20% DMSO and reaction buffer (50 mM MES (6.5), 100 mM CaCl_2)
770 and 20% DMSO (v/v) for a total of 2 h. SagB-SpdC (3 μM) was added to the mixture and
771 then incubated for approximately 8 hours. Enzymes were heat inactivated at 95°C for 5
772 minutes. After cooling reactions to room temperature, ColM (1 mg mL^{-1}) was added to the
773 mixture and incubated for approximately 3 hours at room temperature²³. Protein was
774 precipitated with equal volume methanol. Dried reactions were then resuspended in 20
775 μL of H_2O .

776 **Glycan strand assay**

777 Overnight cultures of wild-type HG003 *S. aureus*, SHM056, and JP132 were
778 diluted 1:100 into 1 L of TSB each and grown at 30 °C for 5 hours. Cells were harvested
779 and sacculi were isolated following a previously published protocol⁴³ with the modification
780 that samples were boiled in SDS for 3 hours. Sacculi were resuspended to 5 mg/mL in

781 500 μ L of 25 mM NaH_2PO_4 pH 7.0 and treated with 100 μ g/mL lysostaphin at 37 $^\circ\text{C}$ with
782 shaking for 9 hours. LytA was then added to 100 μ g/mL and shaking continued at 37 $^\circ\text{C}$
783 for another 14 hours. Enzymes were heat inactivated at 95 $^\circ\text{C}$ for 5 min. Proteins were
784 precipitated with an equal volume of MeOH and removed by centrifugation. To label
785 glycans, we adapted methods previously published⁴⁴. Dried samples were resuspended
786 in 25 μ L of 1 M 2-methylpyridine borane complex in DMSO and 25 μ L of 200 mM 8-
787 aminonaphthalene-1,3,6-trisulfonic acid in 15% acetic acid. Reactions were incubated at
788 room temperature overnight protected from light. Reactions were quenched with 450 μ L
789 of H_2O at room temperature for 1 hr, and an equal volume of MeOH was added. After
790 spinning down, the supernatants were removed to new tubes and dried. Dried samples
791 were resuspended in 50 μ L of 1x loading buffer (125 mM Tris-tricine pH 8.2, 10% glycerol)
792 and loaded on a 20% polyacrylamide gel, which ran for 9 hours at 25 mA. The gel was
793 visualized under UV light at 365 nm.

794 **Crystallization of SagB-SpdC¹⁻²⁵⁶ and data collection**

795 For crystallization trials, SagB-SpdC¹⁻²⁵⁶ was purified as described above. Freshly
796 purified SagB-SpdC¹⁻²⁵⁶ was concentrated to 35-40 mg/ml and immediately reconstituted
797 into lipidic cubic phase by mixing protein and monoolein (Hampton Research) at a 1:1.5
798 ratio by mass, using the coupled syringe method²⁷. All samples were mixed at least 100
799 times prior to crystallization trials. The resulting mixture was dispensed onto glass plates
800 in 35-50 nL drops, then overlaid with 600 nL precipitant solution using an NT8 robot
801 (Formulatrix). Crystals of SagB-SpdC¹⁻²⁵⁶ were grown in precipitant solution containing
802 24-32% PEG400, 500 mM $(\text{NH}_4)_2\text{SO}_4$, and 100mM sodium acetate or sodium citrate pH
803 4.4-5.0; at higher pH crystallization required higher concentrations of PEG400. Most

804 crystals appeared within 36 hours of drop setting and were full-grown in 3-7 days. Crystals
805 were harvested using mesh loops and flash-frozen in liquid nitrogen.

806 Diffraction data were collected at Argonne National Laboratory using NE-CAT
807 beamlines 24-ID-C and 24-ID-E. Two rounds of grid scanning with large and then small
808 beam size were used to locate crystals on the mesh and then precisely determine their
809 positions. All data were collected at 0.979 Å. Datasets were collected 0.2-s exposure and
810 a 0.2° oscillation angle. The presence of multiple crystals on the mesh prevented the
811 collection of full datasets from individual crystals. Data were indexed and integrated in
812 XDS⁴⁵; the SagB-SpdC crystals belonged to the C2 space group. Diffraction data was
813 processed using structural biology software accessed through the SBGrid consortium⁴⁶.
814 Partial datasets from five well-diffracting crystals were then scaled and merged using the
815 CCP4 suite⁴⁷ program AIMLESS⁴⁸.

816 **Structure determination and refinement**

817 The structure was determined by molecular replacement in Phaser using an
818 unpublished structure of the soluble domain of SagB (PDB# 6FXP)^{20,49}. We attempted to
819 place SpdC by molecular replacement using models prepared from the structure of
820 *Methanococcus maripaludis* CAAX protease Rce1 (PDB# 4CAD, 20% sequence identity
821 to SpdC)⁵⁰, but no good solutions were found. Following placement of soluble SagB, only
822 weak density was visible for the transmembrane helices of the complex; those that were
823 clearest were initially modeled as poly-alanine helices using Coot^{51,52}. After one round of
824 automated refinement using phenix.refine⁵³, placement of all nine transmembrane helices
825 was possible, but residue identities were not obvious. Initial assignment was made by
826 sequence alignment and comparison to the structure of Rce1, which appeared to have a

827 similarly threaded transmembrane domain. Density for sidechains in the transmembrane
828 domain became much clearer after several rounds of manual building and automated
829 refinement, and simulated annealing composite omit maps were used to check for model
830 bias and correct errors in the register throughout the process. Towards the end of
831 refinement, a region of clear density remained present at a crystallographic interface
832 between two copies of SagB near residues 38-45 and appeared to be a peptide forming
833 a continuous β -sheet with the two copies of SagB. This peptide is on the unit cell edge
834 but does not appear to be part of either protein; we think it is likely FLAG peptide that
835 carried through the purification and may orient either direction at this interface. Water
836 molecules, sulfate ions, PEG molecules were also added near the end of refinement.
837 Structure quality was assessed using MolProbity⁵⁴, and figures were prepared using
838 PyMOL.

839 **Additional References:**

- 840 29 Qiao, Y. *et al.* Detection of lipid-linked peptidoglycan precursors by exploiting an unexpected
841 transpeptidase reaction. *J Am Chem Soc* **136**, 14678-14681, doi:10.1021/ja508147s (2014).
842 30 Rebets, Y. *et al.* Moenomycin resistance mutations in *Staphylococcus aureus* reduce
843 peptidoglycan chain length and cause aberrant cell division. *ACS Chem Biol* **9**, 459-467,
844 doi:10.1021/cb4006744 (2014).
845 31 Welsh, M. A. *et al.* Identification of a Functionally Unique Family of Penicillin-Binding Proteins. *J*
846 *Am Chem Soc* **139**, 17727-17730, doi:10.1021/jacs.7b10170 (2017).
847 32 Schaefer, K., Owens, T. W., Kahne, D. & Walker, S. Substrate Preferences Establish the Order of
848 Cell Wall Assembly in *Staphylococcus aureus*. *J Am Chem Soc* **140**, 2442-2445,
849 doi:10.1021/jacs.7b13551 (2018).
850 33 Flores-Kim, J., Dobihal, G. S., Fenton, A., Rudner, D. Z. & Bernhardt, T. G. A switch in surface
851 polymer biogenesis triggers growth-phase-dependent and antibiotic-induced bacteriolysis. *Elife* **8**,
852 doi:10.7554/eLife.44912 (2019).
853 34 Coe, K. A. *et al.* Comparative Tn-Seq reveals common daptomycin resistance determinants in
854 *Staphylococcus aureus* despite strain-dependent differences in essentiality of shared
855 cell envelope genes. *bioRxiv* (2019).
856 35 Kato, F. & Sugai, M. A simple method of markerless gene deletion in *Staphylococcus aureus*. *J*
857 *Microbiol Methods* **87**, 76-81, doi:10.1016/j.mimet.2011.07.010 (2011).
858 36 Do, T. *et al.* *Staphylococcus aureus* cell growth and division are regulated by an amidase that trims
859 peptides from uncrosslinked peptidoglycan. *Nat Microbiol* **5**, 291-303, doi:10.1038/s41564-019-
860 0632-1 (2020).
861 37 Lee, W. *et al.* Antibiotic Combinations That Enable One-Step, Targeted Mutagenesis of
862 Chromosomal Genes. *ACS Infect Dis* **4**, 1007-1018, doi:10.1021/acsinfecdis.8b00017 (2018).

- 863 38 Pang, T., Wang, X., Lim, H. C., Bernhardt, T. G. & Rudner, D. Z. The nucleoid occlusion factor Noc
864 controls DNA replication initiation in *Staphylococcus aureus*. *PLoS Genet* **13**, e1006908,
865 doi:10.1371/journal.pgen.1006908 (2017).
- 866 39 Do, T. *et al.* The cell cycle in *Staphylococcus aureus* is regulated by an amidase that controls
867 peptidoglycan synthesis. *bioRxiv*, doi:10.1101/634089 (2019).
- 868 40 Bertsche, U. *et al.* Interaction between two murein (peptidoglycan) synthases, PBP3 and PBP1B,
869 in *Escherichia coli*. *Mol Microbiol* **61**, 675-690, doi:10.1111/j.1365-2958.2006.05280.x (2006).
- 870 41 Barrett, D. *et al.* Analysis of glycan polymers produced by peptidoglycan glycosyltransferases. *J*
871 *Biol Chem* **282**, 31964-31971, doi:10.1074/jbc.M705440200 (2007).
- 872 42 Lebar, M. D. *et al.* Forming cross-linked peptidoglycan from synthetic gram-negative Lipid II. *J Am*
873 *Chem Soc* **135**, 4632-4635, doi:10.1021/ja312510m (2013).
- 874 43 Kuhner, D., Stahl, M., Demircioglu, D. D. & Bertsche, U. From cells to muropeptide structures in 24
875 h: peptidoglycan mapping by UPLC-MS. *Sci Rep* **4**, 7494, doi:10.1038/srep07494 (2014).
- 876 44 Jackson, P. The use of polyacrylamide-gel electrophoresis for the high-resolution separation of
877 reducing saccharides labelled with the fluorophore 8-aminonaphthalene-1,3,6-trisulphonic acid.
878 Detection of picomolar quantities by an imaging system based on a cooled charge-coupled device.
879 *Biochem J* **270**, 705-713, doi:10.1042/bj2700705 (1990).
- 880 45 Kabsch, W. Xds. *Acta Crystallogr D Biol Crystallogr* **66**, 125-132,
881 doi:10.1107/S0907444909047337 (2010).
- 882 46 Morin, A. *et al.* Collaboration gets the most out of software. *Elife* **2**, e01456,
883 doi:10.7554/eLife.01456 (2013).
- 884 47 Winn, M. D. *et al.* Overview of the CCP4 suite and current developments. *Acta Crystallogr D Biol*
885 *Crystallogr* **67**, 235-242, doi:10.1107/S0907444910045749 (2011).
- 886 48 Evans, P. R. & Murshudov, G. N. How good are my data and what is the resolution? *Acta*
887 *Crystallogr D Biol Crystallogr* **69**, 1204-1214, doi:10.1107/S0907444913000061 (2013).
- 888 49 McCoy, A. J. *et al.* Phaser crystallographic software. *J Appl Crystallogr* **40**, 658-674,
889 doi:10.1107/S0021889807021206 (2007).
- 890 50 Manolaridis, I. *et al.* Mechanism of farnesylated CAAX protein processing by the intramembrane
891 protease Rce1. *Nature* **504**, 301-305, doi:10.1038/nature12754 (2013).
- 892 51 Emsley, P. & Cowtan, K. Coot: model-building tools for molecular graphics. *Acta Crystallogr D Biol*
893 *Crystallogr* **60**, 2126-2132, doi:10.1107/S0907444904019158 (2004).
- 894 52 Emsley, P., Lohkamp, B., Scott, W. G. & Cowtan, K. Features and development of Coot. *Acta*
895 *Crystallogr D Biol Crystallogr* **66**, 486-501, doi:10.1107/S0907444910007493 (2010).
- 896 53 Adams, P. D. *et al.* PHENIX: a comprehensive Python-based system for macromolecular structure
897 solution. *Acta Crystallogr D Biol Crystallogr* **66**, 213-221, doi:10.1107/S0907444909052925 (2010).
- 898 54 Chen, V. B. *et al.* MolProbity: all-atom structure validation for macromolecular crystallography. *Acta*
899 *Crystallogr D Biol Crystallogr* **66**, 12-21, doi:10.1107/S0907444909042073 (2010).
- 900